Check for updates

Slightly congested amino terminal dendrimers. The synthesis of amide-based stable structures on a large scale†

Anjara Morgado, [a,b] Francisco Najera, [a,b] Anna Lagunas, [c,d] Josep Samitier, [c,d,e] Yolanda Vida [*a,b] and Ezequiel Perez-Inestrosa [*a,b]

Nowadays, amino terminal dendrimers are appealing materials for biological applications due to their multivalence and the versatile conjugation of the amino groups. However, the high reactivity of these terminal groups can be decreased by steric hindrance, limiting their possible bioapplications. Herein, we report the divergent synthesis of slightly sterically hindered amino terminal polyamide dendrimers. A simple and unique AB_2 scaffold has been chosen to build the dendritic structures, where only amide bonds have been used as the connecting unit. The 1–7 relative positions of the amino groups in the AB_2 monomers avoid the steric congestion of the macromolecules, allowing the construction of robust dendrimers up to the fifth generation. The construction of the dendrimers is based on two well-established reactions, using simple and cheap reactants, with yields above 90% on a gram scale and easy purification procedures. This synthetic methodology constitutes an easy and efficient way for the preparation of stable and aqueous soluble dendrimers on a gram scale, representing a substantial improvement over the synthesis of this kind of aliphatic polyamide amino terminal dendrimer. The prepared structures were completely characterized and evaluated by size exclusion chromatography, diffusion ordered spectroscopy and atomic force microscopy to determine their size. Molecular dynamics simulations were also carried out and the values obtained were consistent with the experimentally determined values.

Introduction

Nowadays, dendrimers are considered one of the best appealing materials for biological applications. The interesting properties of dendritic structures arise from their scaling size and the number of terminal functional groups with generations. Their hyperbranched and well-defined structure allows dendrimers to confine a large number of functional groups in a relatively small space, and this controlled multivalence makes dendrimers unique for certain bioapplications.[1] Among all the

dendrimers established, those with amino-terminal aqueous solubility are an excellent alternative for biological applications. Out of these, the most suitable and available are polypropylenimine (PPI),[2] poly(L-lysine) (PLL),[3] polyamidoamine (PAMAM)[4] and a modification of polyester (2,2-bis(methylol) propionic acid, bis-MPA).[5] Among all, PAMAM is probably the most extensively used.[6] Nonetheless, limitations regarding the synthesis, quality or stability of these dendrimers have been previously reported. While PLL is different from the others in its asymmetry, retro-Michael reactions and intramolecular cyclization may cause defects in the structures of PAMAM and PPI; it is reported for the former that only 29% is defect-free up to generation five.[7–9] Polyester (bis-MPA) dendrimers avoid such kinds of drawbacks; however, their lack of stability due to hydrolysis reactions may be a problem for certain applications.[5]

In recent years, the chemistry of dendrimers has proliferated with the introduction of different methodologies, with the aim to optimize and accelerate the construction of these complex macromolecules. The first divergent and convergent approaches, proposed by Vögtle,[2] Tomalia,[10] Newkome,[11] and Fréchet,[12] laid the basis for the synthesis of dendrimers, independently or in combination.[4,13–15] These are now complemen-

[a]*Universidad de Málaga - IBIMA, Dpto. Química Orgánica, Campus de Teatinos s/n, 29071 Málaga, Spain. E-mail: inestrosa@uma.es, yolvida@uma.es*
[b]*Centro Andaluz de Nanomedicina y Biotecnología-BIONAND. Parque Tecnológico de Andalucía, c/Severo Ochoa, 35, 29590 Campanillas, Málaga, Spain*
[c]*Institute for Bioengineering of Catalonia (IBEC), Barcelona Institute of Science and Technology (BIST), 08028 Barcelona, Spain*
[d]*Biomedical Research Networking Center in Bioengineering, Biomaterials, and Nanomedicine (CIBER-BBN), 28029 Madrid, Spain*
[e]*Department of Electronics and Biomedical Engineering, University of Barcelona (UB), 08028 Barcelona, Spain*
†Electronic supplementary information (ESI) available: ^{1}H, ^{13}C, COSY and HSQC spectra of all of the described compounds, DOSY NMR experiments, AFM experiments and theoretical calculations. See DOI: 10.1039/d1py00667c

ted with new procedures, such us accelerated strategies, which focus on reducing the number of reaction steps.[16] To achieve this, orthogonal and chemoselective reactions are used, where click reactions play the most important role.[17] The one-pot reaction strategy has also been used in the synthesis of dendrimers,[18,19] and has recently been applied to obtain up to four generation dendrimers using four chemoselective reactions.[20] However, even though the synthesis time is reduced, the preparation of up to four different monomers with different functionalities is required.

Previously, we reported new classes of amino-terminal dendrimers by applying different methodologies. Bisaminoalkylpolyamide dendrimers (BAPAD) were synthesized using 3,3′-diaminopivalic acid as a scaffold, following a divergent approach.[21] However, the inherent structure of the dendrimers, together with the synthetic methodology proposed, allows the construction of the dendrimers only until the third generation.[21] This could probably be caused by a back-folding of the terminal groups, which decreases dramatically their reactivity. This setback can partially be solved by changing the core of the dendrimer, obtaining thus the dendrimer until generation four.[22] Using the same scaffold, but changing the synthetic strategy completely, we develop a new class of amino terminal dendrimers taking advantage of click reactions. Thus, dendrons up to generation 3 were prepared and used to couple with different multifunctional groups. In this convergent approach, large quantities of dendrons were obtained with more than 85% yield. Different dendrimers were also prepared using cores of different multiplicities, demonstrating the potential of this methodology for the assembly of dendrimers with a controlled shape and number of amino terminal groups.[23]

These amide-based dendritic structures are completely stable, aqueous soluble and versatile enough to be used in different bioapplications. Thus, dendrons based on this structure were used as platforms in diagnosis tests of allergic reactions to drugs.[24] The dendritic moieties have also been used as scaffolds for the covalent immobilization of bioactive peptides in titanium disks, increasing the biocompatibility of oral titanium implants.[25] Furthermore, the insertion of these dendritic scaffolds into Pt(II) complexes endows them with unique properties such as aqueous solubility, shielding from quenching by dioxygen, and binding to bacterial surfaces, opening the way for the development of new phosphorescent biomarkers with promising properties.[26]

Despite the versatility of the system, only relatively low generations of dendrimers can be prepared on a large scale. Another aspect to improve is the proximity of the terminal amino groups. The use of 3,3′-diaminopivalic acid as a scaffold promotes a 1–3 relative position between the terminal amino groups in the dendrimers. The proximity of the terminal groups may promote an extremely dense surface packing that, together with their back-folding, can be responsible for a steric hindrance inhibited reaction rate.[22,27] Above this critical point, the lower reactivity of the terminal amino groups can be responsible not only for the limited success in obtaining higher-generation dendrimers, but may also have contributed towards incomplete functionalization of the amino terminal groups necessary for certain bioapplications.

Herein, we report the divergent synthesis of a less sterically hindered amino terminal polyamide dendrimer. Based on the excellent properties of our previous developments, only amide bonds were used in the construction of these new dendritic architectures. 5-Amino-2-(3-aminopropyl)pentanoic acid has been chosen as a single and simple AB_2 scaffold to build the dendrimer. The presence of two amino groups in 1–7 relative positions resulted in the synthesis of slightly congested structures, while the carboxylic acid acted as the connecting unit. Using ethylenediamine (EDA) as a core, two steps are involved in increasing the dendrimer generation: amide formation and amine deprotection. Both are well-established procedures, using simple and cheap reactants, with yields above 90%, on a gram scale and easy purification procedures. The use of a unique scaffold in the synthesis also avoids the tedious work to construct a family of different monomers, while simplifying the structure of the final dendrimer. This synthetic methodology constitutes an easy and efficient way for the preparation of stable and aqueous soluble dendrimers on a gram scale in higher generations. The prepared structures were completely characterized and evaluated by size exclusion chromatography (SEC), diffusion-ordered spectroscopy (DOSY) and atomic force microscopy (AFM) to determine their size. Molecular dynamics simulations (MDS) were also carried out, with the values consistent with the experimentally determined values.

Experimental

All reactions were performed using commercially available reagents and solvents from the manufacturer without further purification. Unless otherwise stated, all reactions were performed in air. Column chromatography and TLC were performed on silica gel 60 (0.040–0.063 mm) using UV light and/or stains to visualize the products. SephadexTM G-10 column chromatography (100 g sephadex in a 5 cm diameter column) and SephadexTM G-10 pre-packed columns were used to purify the final dendrimers. Chemicals were purchased from Sigma-Aldrich (di-tert-butyl-dicarbonate, N-methylmorpholine, 1-hydroxybenzotriazole), Alfa Aesar (Amberlyst A-26, Celite, sodium hydride, di-tert-butyl malonate, ethylenediamine, 4 M hydrochloric acid : dioxane) or panreac (triethylamine, acetic acid, hydrochloric acid, sodium hydroxide) and used without further purification, unless otherwise indicated. Water was purified with a Mili-Q purification system from Millipore.

^{1}H-NMR and ^{13}C-NMR experiments were performed in the indicated deuterated solvent at 25 °C on a Bruker Ascend 400 MHz spectrometer. Proton chemical shifts (δ) are reported with the solvent resonance employed as the internal standard CDCl$_3$ δ 7.26, DMSO-d_6 δ 2.50 and D$_2$O δ 4.79. Carbon chemical shifts are reported in ppm with the solvent resonance as the internal standard CDCl$_3$ δ 77.16 and DMSO-d_6 δ 39.52. ^{1}H-RMN data are reported as follows: chemical shift, multi-

plicity, coupling constants (Hz) and integration. The HRMS (Electrospray Ionization Time of Flight, ESI-TOF mass spectrometry (MS)) was performed on a high resolution mass spectrometer Orbitrap, Q-Exactive (Thermo Fisher Scientific, Waltham, MA, USA), in either positive or negative ion mode. Matrix-Assisted Laser Desorption Ionization Time of Flight Mass Spectrometry (MALDI-TOF MS) was used to measure the mass of the dendritic materials, and it was conducted on a Bruker MicroFlex MALDI-TOF MS. The obtained spectra were analyzed with FlexAnalysis Bruker Daltonics versión. The detector mass range was set from 100 to 5000 Da, depending on the size of the dendritic structure analysed. A solution of 10 mg mL^{-1} of dithranol (DIT) or 2,5-dihydroxybenzoic acid (DHB) was used as the matrix.

HPLC chromatograms were obtained using a JASCO HPLC system equipped with a refractive index (RI) detector and a size exclusion column (SEC) Styragel® HR 4E DMF at room temperature using DMF LiCl 10 mM as the mobile phase. The concentration of the samples was 1 mg mL^{-1} and the flow rate was 0.7 mL min^{-1}.

General procedure for deprotection of terminal amine groups

Gx-NHBoc (1 eq.) was dissolved in THF (10 mL) and the solution was cooled in an ice-water bath. 4 M HCl in dioxane (10 mL) was added dropwise and the mixture was stirred until the reaction was completed. Afterwards, the solvent was evaporated under vacuum to obtain the products in a quantitative way. The compounds were purified by size-exclusion chromatography.

General procedure for dendrimer growth reactions

Amino terminal dendrimer **Gx** (1 eq.) was dissolved in the minimum volume of methanol. Amberlyst A-26(OH) ion exchange resin (250 mg mmol^{-1} of the amine group) was added and left in a shaker for one hour. Afterwards, the resin was removed by filtration through MeOH-pre-wetted Celite and the solvent was removed under vacuum. The amine-free terminal dendrimer was dissolved in dry DMF under a nitrogen atmosphere, **1** (1.1 eq. per amine group) and *N*-methylmorpholine (1.5 eq. per amine group) were added and the mixture was stirred at room temperature. Once finished, the solvent was removed. The crude was dissolved in dichloromethane (60 mL) and washed with water (2 × 30 mL) and saturated NaHCO$_3$ solution (2 × 30 mL). The organic layer was dried over MgSO$_4$ and the solvent was removed. The product was purified by precipitation in hexane.

DOSY nuclear magnetic resonance (NMR) experiments

The samples were prepared in deuterium oxide at a concentration between 0.5 and 2 mM (within the infinite dilution range for similar samples at 0.1–2.1 mM).[28] For all samples, DOSY experiments were performed with decreasing concentrations until no differences between the diffusion coefficients were observed. The experiments have been performed on a Bruker AscendTM 400 MHz spectrometer equipped with a 5 mm BBFOPLUS probe with a 2H "lock" channel and *Z* gradi-

ent. The spectrometer is also equipped with a control temperature unit prepared to work at temperatures ranging from 0 °C to +50 °C. The gradient strength was calibrated by measuring the diffusion rate of pure water of residual protons in D$_2$O. All experiments were conducted at 300 K. The samples were allowed to equilibrate for no less than 15 min. To determine the diffusion rates, a 2D sequence using double stimulated echo for convection compensation and a LED using bipolar gradient pulses for diffusion were used. The diffusion coefficients (*D*) were determined from the slope of the Stejskal–Tanner plot, which relates it to the signal intensity through the following equation:

$$\ln\left(\frac{I}{I_0}\right) = -\gamma^2\delta^2 G^2\left(\Delta - \frac{\delta}{3}\right)D,$$

where *I* is the integral of the peak area at a given value of *G*, I_0 is the integral of the peak area at *G* = 0, *G* is the gradient field strength, *γ* is the gyromagnetic ratio, *δ* is the gradient duration and Δ is the time between the gradient pulses.[29] The diffusion coefficients determined were used to calculate the hydrodynamic radius *via* the Stokes–Einstein equation:

$$R_{\rm h} = K_{\rm B}T/6\pi\eta D,$$

where K_B is the Boltzmann constant, *T* is the temperature and *η* is the viscosity of the solution (1.0963 cP for D2O viscosity).[28]

Dendrimer deposition and AFM analysis

Atomically flat Au(111) single-crystal disks of 10 mm diameter and 1 mm thickness (MaTecK) were flame annealed prior to use and incubated with 150 μL of an aqueous solution of the dendrimer at 1.5×10^{-7}, 1.1×10^{-7} and 7.2×10^{-8} w/w for **G3**, **G4** and **G5**, respectively. All solutions were prepared in pure water (18 MΩ cm^{-1} <4 ppb TOC Milli-Q, Millipore) and sonicated for 10 min before use. Dendrimer stock solutions were used within 6 months of preparation.

Substrates were imaged by AFM using a Dimension 3100 AFM instrument (Veeco Instruments) operated in tapping mode in air. Silicon AFM probes (Budget Sensors) with a spring constant *k* = 40 N m^{-1} and a resonant frequency *ν* = 300 kHz were used. At least 4 areas in two independent substrates were analyzed. AFM images were processed with WSxM software.[30]

Molecular dynamics simulations

Simulations were performed in water as an explicit solvent using the AMBER12 MD software package.[31] Briefly, AMBER force field (parm99) parameters have been used and the General Atom Force Field (GAFF) parameters to include parameters when needed.[32] Initial dendrimer conformations were made using the Dendrimer Building Tool (DBT).[33] The systems were minimized and then heated to 300 K over 40 ps. Nonbonded interactions were cutoff at 9 Å. Time steps of 2 fs were carried out employing the SHAKE routine.[34] Simulations were run at physiological pH (7.4) in the NPT ensemble (300 K and 1 atm). Dendrimers were equilibrated for 2 ns and starting from these configurations were performed production runs of

20 ns trajectories. Trajectory analyses were performed using the Amber modules *ptraj* and *cpptraj*. Snapshots from the trajectories within this paper were produced with VMD software.[35] The details of the molecular dynamics simulations are thoroughly detailed in the ESI.†

Results and discussion

In general, amino terminal dendrimers are excellent scaffolds for a series of bioapplications where the conjugation of such groups with bioactive molecules plays a crucial role. These terminal groups impart aqueous solubility to the dendrimers, while can also become positively charged, essential aspects for some request. One more important feature to take into account is stability, a critical aspect in some applications where the role of the dendrimer is a carrier vehicle. In our dendrimer design, an exclusive amide based scaffold has been selected to avoid stability problems or protonation of internal amino groups that could alter the size or the charge. A unique monomer was carefully chosen to simplify not only the synthesis, but also the structure of the resulted dendrimer. A divergent approach was designed to build the dendritic structures, with just a couple of well-known, effective, easy and cheap reaction steps.

Synthesis

For the synthesis of these amide based structures, a simple AB_2 type monomer was designed. In order to achieve a higher separation between amine terminal groups, 5-amino-2-(3-aminopropyl)pentanoic acid was selected as a platform to build the dendrimers. This will arrange the terminal amino groups in a 1,7 relative position, achieving less steric hindrance than in previously prepared BAPAD[21] or clicked dendrimers,[23] where the amino groups were in a 1,3 relative position.

The presence of a carboxylic acid and two amino groups in the selected AB_2 monomer will ensure that all connections will be exclusively amide bonds. 5-Amino-2-(3-aminopropyl)pentanoic acid was prepared according to procedures previously described (detailed synthetic protocols are described in the ESI†).[36] For the growth of the dendrimers, the amine groups of 5-amino-2-(3-aminopropyl)pentanoic acid were protected with *tert*-butoxycarbonyl (Boc) derivatives and the carboxylic group was activated using 1-hydroxybenzotriazole (HOBt), obtaining **1** (Scheme 1) in >90% yield. A simple nucleus (EDA) has been selected to build the dendrimers in a divergent way. Two iterative steps of amidation/deprotection reactions produced consistently high generations of dendrimers in up to 90% yield in all cases on a multigram scale.

Amidation reactions were carried out with a slight excess of **1** for lower generations; nevertheless, to ensure the reaction of all branches of the dendrimers, refreshing with different
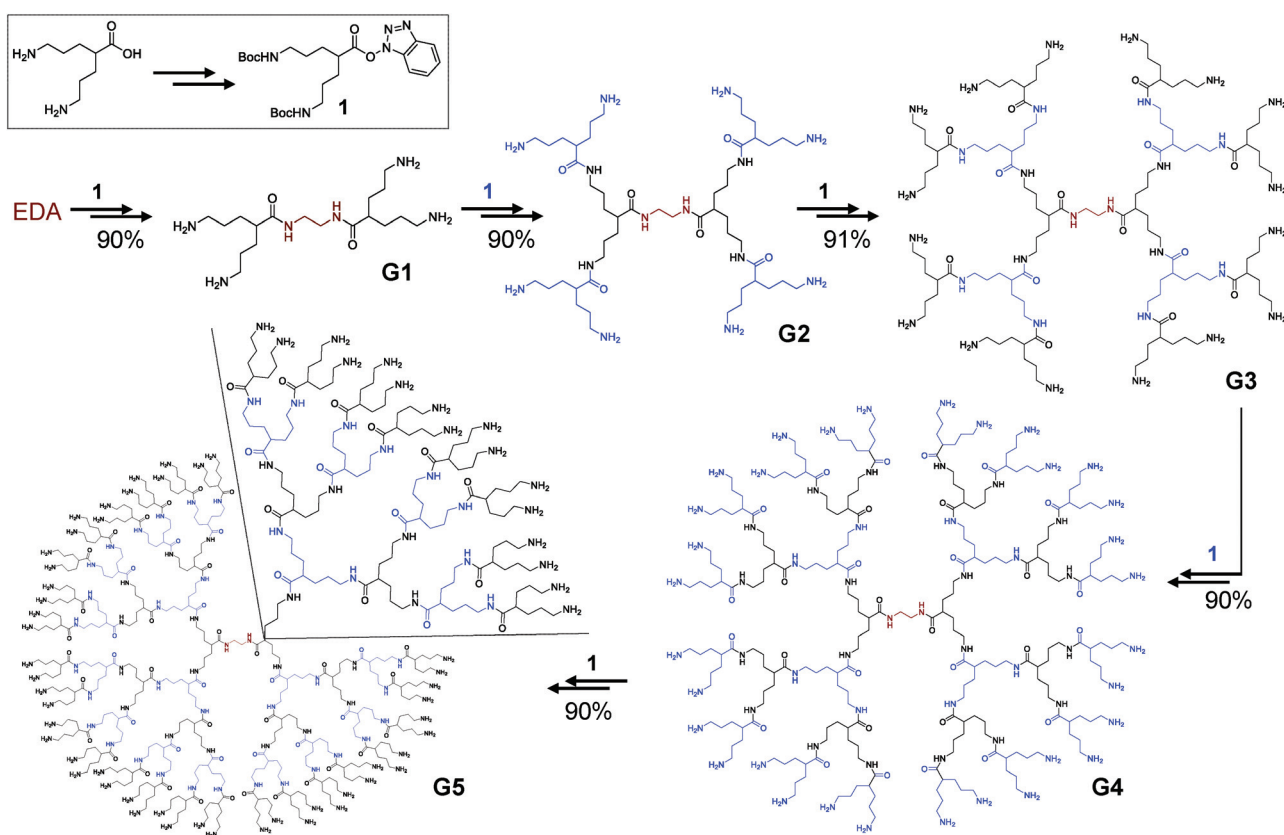
Scheme 1 Synthesis of all-amide dendrimers up to the 5th generation. Growth steps consist of an amidation reaction (*N*-methylmorpholine, DMF, r.t.; yield indicated for each reaction) followed by the deprotection of the terminal amino groups (4 M HCl in dioxane, THF; quantitative).

amounts of **1** was needed when increasing generation. For an effective coupling, a pre-treatment with an Amberlyst A-26(OH) ion exchange resin has been made to the dendrimers to guarantee that all terminal amino groups were in a non-protonated form. The amidation reactions afforded Boc-protected dendrimers (**Gx-NHBoc**) in excellent yields. It is noteworthy that no further purifications were needed for **G1-NHBoc** and **G2-NHBoc**. For higher generations, precipitation in hexane yielded pure compounds in excellent yields (Scheme 1). No chromatography was needed for the purification of **Gx-NHBoc**, avoiding tedious and time consuming procedures. The deprotection of the terminal amino groups was carried out under acidic conditions, and all amino terminal dendrimers were filtered by size-exclusion chromatography. **G1–5** dendrimers were obtained in an almost quantitative way in all cases.

Characterization

The structures of **G1-5** dendrimers were analyzed by nuclear magnetic resonance (NMR) spectroscopy. ^{1}H-NMR spectra in DMSO-d_6 are shown in Fig. 1. For **G1**, protons corresponding to the ethylene core (EDA in Fig. 1) can be clearly distinguished as a singlet at 3.13 ppm. Regarding the branching moieties, protons corresponding to the adjacent methylenes to the amino terminal groups (d_1 in Fig. 1) appear as a multiplet centered at 2.75 ppm. The broad signal at 2.38 ppm corresponds to the proton adjacent to the carbonyl group (a_1 in Fig. 1). Finally, protons corresponding to the rest of methylenes (b_1 and c_1 in Fig. 1) appear as multiplets. Methylene b_1 protons are constitutionally non-equivalent and present different chemical shifts, appearing at both 1.33 ppm and 1.51 ppm (together with c_1 protons). The same behavior was also observed in BAPAD type dendrimers.[21]

Growth in a generation can be clearly observed in the ^{1}H-NMR spectra of **G2**. The signal corresponding to d_1 shifted to 3.08 ppm, indicating the reaction of the amino groups of **G1**, forming amide bonds in **G2**. New signals appear overlapping those corresponding to **G1**, causing a widening of the peaks. The most relevant is the new signal at 2.74 ppm, corres-
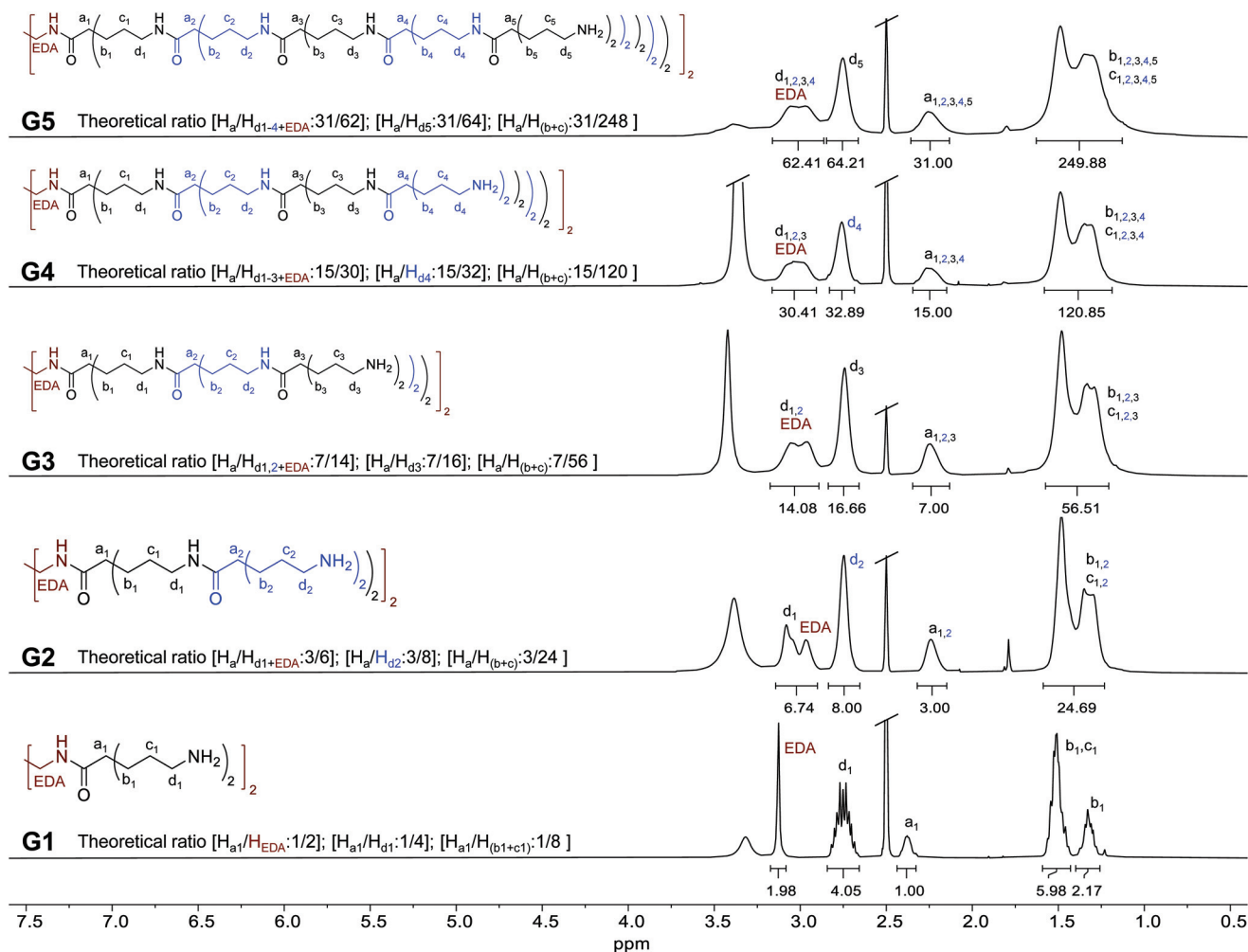

Fig. 1 ^{1}H-NMR spectra in DMSO-d_6 of **G1–5** dendrimers. Integral values refer to the numbers of H_a protons in half dendrimers. The theoretical relationship between the numbers of H_a protons with respect to each type of signal is indicated for each dendrimer. Integral values refer to half dendrimers for clarity.

ponding to the new methylenes adjacent to the new terminal amino groups (d_2 in Fig. 1). The same trend is observed in the ^{1}H-NMR spectra for higher generation dendrimers. A new layer involves the overlapping of internal d signals (as the formation of amide bonds involved an upper field shift of the signals of the previous generation d-terminal). The broadening of these signals also implies an overlap with the signal of the ethylene core (EDA) protons, while the new generation d protons (d-terminal) appear at around 2.75 ppm. In all cases, the peaks corresponding to a, b and c protons overlap, promoting a broadening of the signals in each generation.

To evaluate the integral values, the signal corresponding to H_a protons has been used as a reference. This value was adjusted to the number of H_a in each dendrimer (we used half dendrimers for clarity, since the number of protons increases significantly with generations). The theoretical ratio between the integral values is indicated in Fig. 1 for each compound. As can be observed, these values correlate very well with the values of the integral in each spectrum (experimental values are indicated under the corresponding signal in Fig. 1). This seems to indicate a complete growth reaction in each case. More details about the NMR characterization of **G1–5** as well as the Boc-protected derivatives can be found in the ESI (Fig. S1 to S56, ESI†). ^{1}H-NMR spectra of an aqueous solution of **G5** kept at 37 °C for one week were also recorded. No differences between both the spectra of **G5** (freshly prepared or after one week) were observed (Fig. S57, ESI†), as may be expected given the stability of these amide-based dendrimers.

MALDI-TOF obtained values for the smaller generation dendrimers correlated well with the theoretical values, verifying their structures (Fig. S58 to S62, ESI†). However, as previously reported, characterization of dendrimers with high molecular weights and charges by MALDI-TOF is extremely difficult.[23,37,38] For **G4-5** no MALDI spectrum could be obtained, probably due to the high lability of the Boc protecting groups (in **Gx-NHBoc**) and the high degree of positive charges (in **G4-5**) during measurements.

Protected **Gx-NHBoc** dendrimers were analyzed by size exclusion chromatography (SEC). SEC chromatograms corroborate the conversions to higher generations, showing bands shifted to lower elution times as generations increased (Fig. 2). For generations up to four, SEC bands show a shoulder at lower elution times (higher molar mass) probably due to the presence of potential aggregates, as has been reported in other cases for generation-4 dendrimers.[20]

Amino terminal obtained dendrimers were examined by diffusion NMR techniques. DOSY (diffusion-ordered spectroscopy) experiments were carried out in D_2O solutions. Decays of the signals were monoexponential in all cases, which is translated into linear Stejskal–Tanner plots (Fig. 3a and Fig. S63 to S67, ESI†).[39] Fig. 3a shows the amplitude decays of dendrimers, where the logarithms of the normalized signal intensities are plotted against the gradient squared. The linear relationship obtained for all samples indicates that they are pure and monodisperse macromolecules. Diffusion coefficients (D) were also determined and used to estimate the size of all dendrimers in solution, by calculating the hydrodynamic radius (R_h) using the Stokes–Einstein equation (Table 1).[28,29]
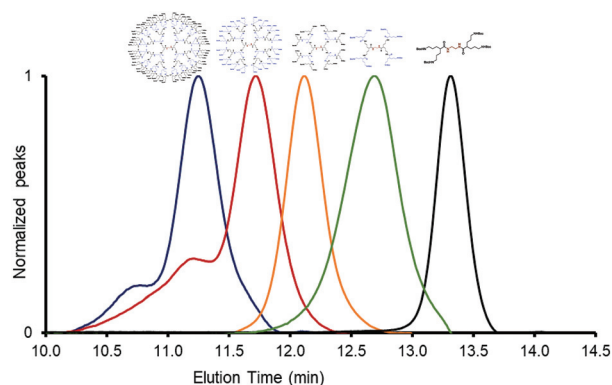

Fig. 2 SEC chromatograms of **Gx-NHBoc** dendrimers, using DMF/LiCl as an eluent and a (SEC) Styragel® HR 4E DMF column at 0.7 mL min^{-1} flow rate. Black (generation 1), green (generation 2), orange (generation 3), red (generation 4) and blue (generation 5).
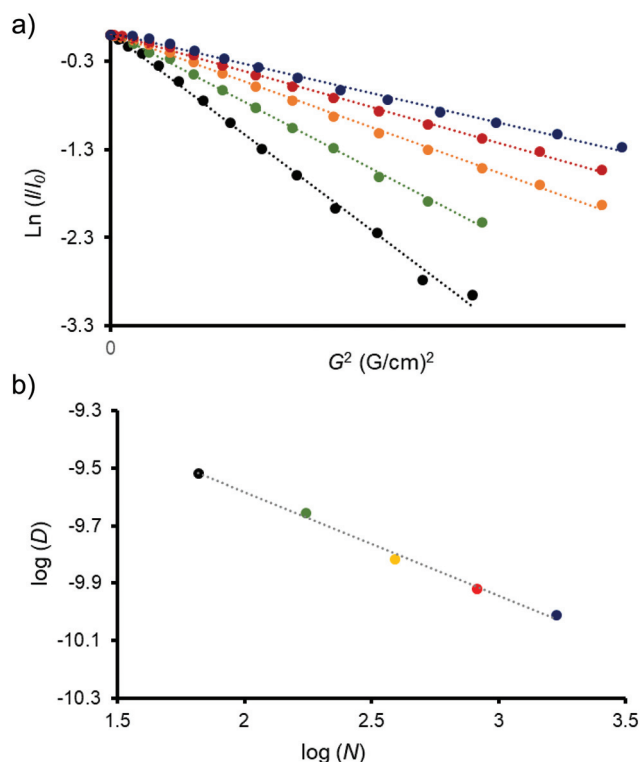

Fig. 3 (a) Stejskal–Tanner plots of the synthesized dendrimers in D_2O. (b) Log–log representation of the diffusion coefficients *versus* the approximate number of atoms for each dendrimer. Values of D were taken from the slopes of the Stejskal–Tanner plots in (a). In both cases black (generation 1), green (generation 2), orange (generation 3), red (generation 4) and blue (generation 5).

As expected, both the diffusion constants and hydrodynamic radius scale with dendrimer generation. **G1** diffused the fastest, at almost three times the rate of **G5** (Table 1), corresponding to the smallest observed R_h. It has been previously reported that the diffusion coefficients of PAMAM dendrimers (up to the fifth generation) scale exponentially with the

Table 1 Data of the prepared amino terminal dendrimers. The diffusion coefficients (D) and hydrodynamic radius (R_h) determined by NMR experiments. The radius of gyration (R_g), aspect ratios (I_z/I_x and I_z/I_y) and asphericities (δ) calculated by MDS[a]

Dendrimer	G1	G2	G3	G4	G5
Formula	$C_{18}H_{40}N_6O_2$	$C_{50}H_{104}N_{14}O_6$	$C_{114}H_{232}N_{30}O_{14}$	$C_{242}H_{488}N_{62}O_{30}$	$C_{498}H_{1000}N_{126}O_62$
Terminal-NH$_2$	4	8	16	32	64
M.W. (gmol^{-1})	372.56	997.47	2247.31	4746.97	9746.30
D (m^2 s^{-1})	3.039×10^{-10}	2.2135×10^{-10}	1.5275×10^{-10}	1.2035×10^{-10}	9.7121×10^{-11}
R_h (Å)	6.59	9.05	13.12	16.65	20.63
R_g (Å)	5.26 ± 0.26	8.06 ± 0.19	11.02 ± 0.24	14.87 ± 0.23	18.81 ± 0.28
I_x/I_y	1.19 ± 0.10	1.53 ± 0.10	1.37 ± 0.09	1.08 ± 0.04	1.26 ± 0.08
I_x/I_z	3.08 ± 0.49	2.05 ± 0.21	1.68 ± 0.12	1.57 ± 0.11	1.58 ± 0.09
δ	0.080 ± 0.016	0.045 ± 0.008	0.024 ± 0.006	0.017 ± 0.005	0.018 ± 0.003

[a] Values averaged over the last 1 ns simulation run taking each snapshot after 1 ps.

number of atoms in the dendrimer structure, following the relation $D \approx N^\alpha$ (where N is the number of atoms and α is a scaling constant).[28,29,39] Fig. 3b shows the log–log relation between D and N in the prepared dendrimers. As can be clearly observed, dendrimers from generations 1 to 5 adjust perfectly in a linear dependence. From the slope, we assume a

scale factor of $\alpha = -0.36$. This value is practically identical to the observed value for the aqueous solutions of PAMAM dendrimers ($\alpha = -0.35$).[28,29]

Amino terminal dendrimers were also analyzed by atomic force microscopy (AFM) by depositing diluted solutions of the dendrimers on (111) gold single-crystal substrates (Fig. 4).[40,41]
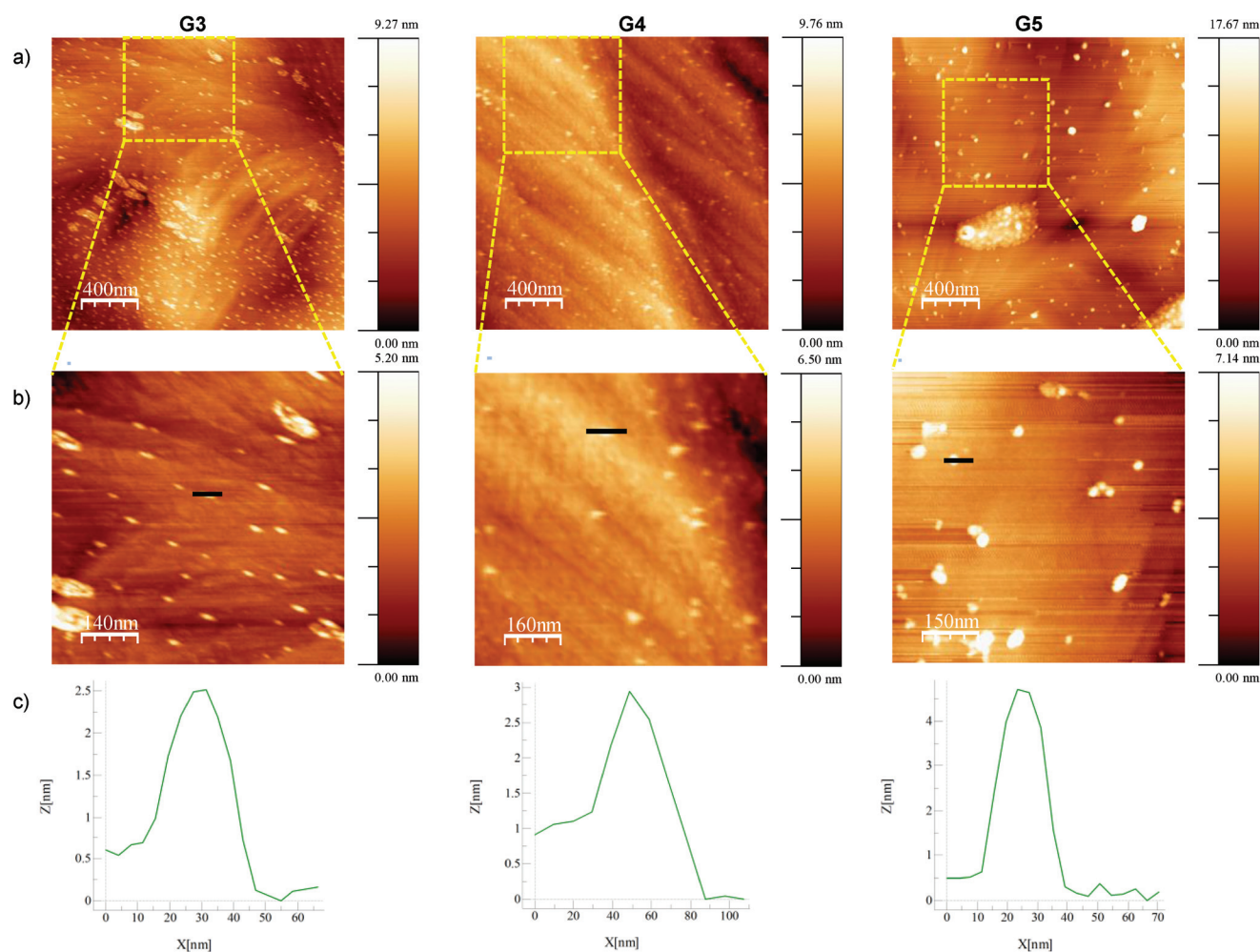
Fig. 4 (a and b) AFM images obtained for **G3**, **G4** and **G5** deposited on (111) gold substrates. Images in (b) correspond to the zoomed-in sections of the dashed areas depicted in (a). (c) High-distance profiles obtained for the representative features selected in (b) (bold black lines).

Isolated dendrimers could mostly be found in the **G3** and **G4** samples, together with some two-dimensional aggregates. Conversely, in **G5** aggregation was predominant, leading to both chains of dendrimers and three-dimensional aggregates (Fig. 4a and Fig. S68 in the ESI†). Analysis of single dendrimers in the zoomed-in sections of the AFM images (Fig. 4b) shows the measured heights of approximately 25, 30 and 45 Å for **G3**, **G4** and **G5** respectively. These values are in concordance with the results observed from DOSY experiments (Table 1).

Molecular dynamics simulations

Molecular models of these dendrimers were built and subjected to molecular dynamic simulations in water as an explicit solvent (Fig. 5). Three different residues were used to define these compounds: the core (COR), the repeating fragment (REP), and the terminal ones (TAM) (Fig. S69, ESI†). The structures obtained from MDS have been analyzed and properties such as the radius of gyration (R_g), the aspect ratio and the asphericities have been calculated (Table 1 and Fig. S76 and S77 in the ESI†).

The radius of gyration obtained from the MDS calculations (Table 1) is in good agreement with the values quantified from the DOSY experiments and shows an increase in the size of these dendrimers from generation 1 to 5.

The aspect ratio of these dendrimers can be inferred from the average of the three principal moments of inertia (I_x, I_y, and I_z in decreasing order). The ratios (I_x/I_y) and (I_x/I_z) are the measures of the eccentricity (minor-major axes ratio) of the ellipsoid shape of the dendrimers. As the generation of dendrimers increases from **G1** to **G5**, the relationship between the I_x/I_y and I_x/I_z values becomes smaller, indicating a change in the shape from ellipsoid to globular. This is also corroborated by the decrease in the asphericity values (Table 1 and Fig. S77†).

The logarithmic linear relationship between the number of atoms ($\log N$) and the radius of gyration ($\log R_g$) points to a
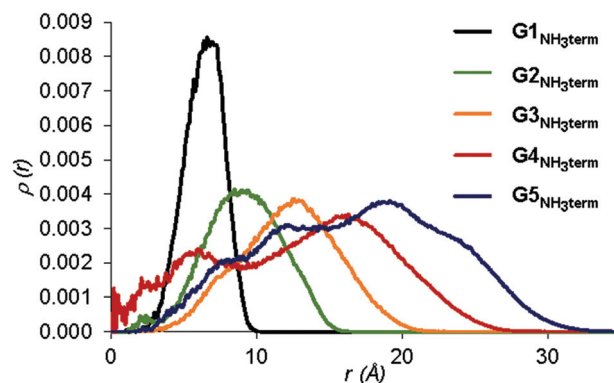

Fig. 6 Radial distribution function of the terminal amino groups in Gn-NH$_{3term}$ using the dendrimer center of mass as a reference. The unit value for $\rho(r)$ is expressed in atoms per Å^3.

space-filling structure and the correlated fractal dimension (d_f) gives an idea of the compactness of the dendrimer series. The size scale found for this dendrimer series is $N \approx R_g^{2.51}$ (d_f = 2.51, Fig. S78, ESI†). This implies that these dendrimers have a more polymeric-like structure than a perfect compact sphere where d_f is 3.[42]

The radial density profiles can describe the atom distribution within the dendrimers. Those corresponding to **G1–5** dendrimer generations are shown in Fig. S79, ESI.† All compounds have the maximum density close to the core of the dendrimers and it decreases towards the edge of the molecule. In **G3** to **G5** dendrimers appears a plateau, corresponding to the REP unit distribution, along the entire molecule decaying slowly at the end. This suggests a region with high localization and low atom mobility, showing a dense dendrimer shell pattern. With each generation, the number of TAM units doubles and the terminal amino groups spread over a larger part of the molecule. This points to a high degree of back-folding (Fig. S79, ESI†), especially for **G4** and **G5** dendrimers where an appreciable distribution of the amino terminal groups can be found close to the core, although with increasing density toward the outer region of the dendrimer (Fig. 6).

The design of these dendrimers present some advantages relative to our previously published BAPAD dendrimers decorated with amino terminal groups.[21] Although both dendrimers present compact structures (similar d_f), those described in this work are slightly larger and more globular (better aspect ratios and less asphericities). Finally, they present less back-folding relative to BAPAD, allowing access to higher generations.

Conclusions

The presented methodology allows the preparation of a new family of stable and aqueous soluble high-generation dendrimers on a gram scale, representing a substantial improvement in the synthesis of aliphatic polyamide amino terminal dendrimers. Our design resulted in the achievement of a high
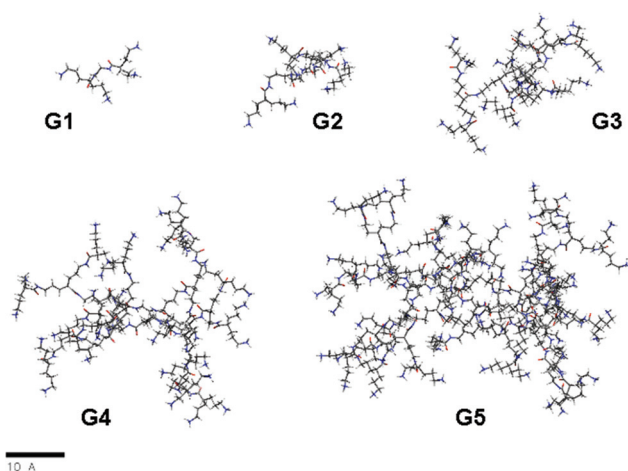

Fig. 5 Snapshots from molecular dynamics simulations of **G1–5**; (to simplify, carbon atoms are depicted in gray, oxygen atoms in red, nitrogen atoms in blue and hydrogens in white).

amount of robust and stable dendrimers using a cheap, easy and efficient synthesis method together with high yields and the avoidance of tedious purification procedures. NMR, SEC, DOSY and AFM techniques were applied to evaluate **G1–5**, and all of them concur with the estimated size of these dendrimers, observing an exponential increase in size with generations. Molecular dynamics simulations (MDS) were also carried out, with the values consistent with the experimentally determined values. **G1–5** are promising scaffolds for applications where the combination of stability, multivalence and efficient conjugation is required.

Author contributions

The manuscript has been written through contributions of all authors. E. Perez-Inestrosa and Y. Vida conceived and designed the experiments. A. Morgado performed the chemical synthesis and analysis of the compounds helped by Y. Vida. F. Najera performed molecular dynamics simulation studies. A. Lagunas and J. Samitier performed the AFM studies.

Conflicts of interest

There are no conflicts to declare.

Acknowledgements

Notes and references

1 R. M. Kannan, E. Nance, S. Kannan and D. A. Tomalia, *J. Intern. Med.*, 2014, **276**, 579–617.

2 E. Buhleier, W. Wehner and F. Vögtle, *Synth.*, 1978, **1978**, 155–158.

3 R. G. Denkewalter, J. F. Kolc, W. J. Lukasavage, K. E. Stroup, R. C. Stewart and A. M. Doernberg, Macromolecular highly branched homogeneous compound, *US Pat.*, 4410688, 1983.

4 D. A. Tomalia and J. M. J. Fréchet, *J. Polym. Sci., Part A: Polym. Chem.*, 2002, **40**, 2719–2728.

5 P. Stenström, E. Hjorth, Y. Zhang, O. C. J. Andrén, S. Guette-Marquet, M. Schultzberg and M. Malkoch, *Biomacromolecules*, 2017, **18**, 4323–4330.

6 Z. Lyu, L. Ding, A. Y. T. Huang, C. L. Kao and L. Peng, *Mater. Today Chem.*, 2019, **13**, 34–48.

7 M. A. Mintzer, M. W. Grinstaff, I. Paetsch, P. Hunold, M. Mahler, K. Shamsi, E. Nagel, C. F. Price, L. J. Clark, J. R. A. Paull, C. K. Fairley, X. Lou and E. W. Meijer, *Chem. Soc. Rev.*, 2011, **40**, 173–190.

8 J. R. Lloyd, P. S. Jayasekara and K. A. Jacobson, *Anal. Methods*, 2016, **8**, 263–269.

9 S. Falkovich, D. Markelov, I. Neelov and A. Darinskii, *J. Chem. Phys.*, 2013, **139**, 064903.

10 D. A. Tomalia, H. Baker, J. Dewald, M. Hall, G. Kallos, S. Martin, J. Roeck, J. Ryder and P. Smith, *Polym. J.*, 1985, **17**, 117–132.

11 G. R. Newkome, Z. Yao, G. R. Baker and V. K. Gupta, *J. Org. Chem.*, 1985, **50**, 2003–2004.

12 C. J. Hawker and J. M. J. Frechet, *J. Am. Chem. Soc.*, 1990, **112**, 7638–7647.

13 F. Vögtle, G. Richardt and N. Werner, *Dendrimer chemistry: Concepts, Synthesis, Properties, Applications*, Wiley-VCH, 2009.

14 D. A. Tomalia, J. B. Christensen and U. Boas, *Dendrimers, Dendrons, and Dendritic Polymers. Discovery, Applications, and the Future*, Cambridge University Press The Edinburgh Building, Cambridge CB2 8RU, UK, 2012.

15 K. L. Wooley, C. J. Hawker and J. M. J. Frechet, *J. Am. Chem. Soc.*, 1991, **113**, 4252–4261.

16 M. V. Walter, M. Malkoch, E. Soderlind, K. Ohshimizu, J. N. Hunt, K. Sivanandan, M. I. Montanez, M. Malkoch, M. Ueda, C. J. Hawker and J. M. DeSimone, *Chem. Soc. Rev.*, 2012, **41**, 4593.

17 G. Franc and A. K. Kakkar, *Chem. Soc. Rev.*, 2010, **39**, 1536–1544.

18 C. Ornelas, J. R. Aranzaes, E. Cloutet and D. Astruc, *Org. Lett.*, 2006, **8**, 2751–2753.

19 L. Brauge, G. Magro, A. M. Caminade and J. P. Majoral, *J. Am. Chem. Soc.*, 2001, **123**, 6698–6699.

20 S. García-Gallego, O. C. J. Andrén and M. Malkoch, *J. Am. Chem. Soc.*, 2020, **142**, 1501–1509.

21 A. J. Ruiz-Sanchez, P. Mesa-Antunez, N. Barbero, D. Collado, Y. Vida, F. Najera and E. Perez-Inestrosa, *Polym. Chem.*, 2015, **6**, 3031–3038.

22 D. Jishkariani, C. M. MacDermaid, Y. N. Timsina, S. Grama, S. S. Gillani, M. Divar, S. S. Yadavalli, R.-O. Moussodia, P. Leowanawat, A. M. Berrios Camacho, R. Walter, M. Goulian, M. L. Klein and V. Percec, *Proc. Natl. Acad. Sci. U.S.A.*, 2017, **114**, E2275–E2284.

23 N. Molina, F. Nájera, J. A. Guadix, J. M. Perez-Pomares, Y. Vida and E. Perez-Inestrosa, *J. Org. Chem.*, 2019, **84**, 10197–10208.

24 P. Mesa-Antunez, D. Collado, Y. Vida, F. Najera, T. Fernandez, M. Torres and E. Perez-Inestrosa, *Polymers*, 2016, **8**, 111.

25 N. Molina, A. González, D. Monopoli, B. Mentado, J. Becerra, L. Santos-Ruiz, Y. Vida and E. Perez-Inestrosa, *Polymers*, 2020, **12**, 770.

26 N. Molina, M. Cnudde, J. A. Guadix, J. M. Perez-Pomares, C. A. Strassert, Y. Vida and E. Perez-Inestrosa, *ACS Omega*, 2019, **4**, 13027–13033.

27 P. G. de Gennes and H. Hervet, *J. Phys., Lett.*, 1983, **44**, 351–360.

28 V. A. Jiménez, J. A. Gavín and J. B. Alderete, *Struct. Chem.*, 2012, **23**, 123–128.

29 M. A. van Dongen, B. G. Orr and M. M. Banaszak Holl, *J. Phys. Chem. B*, 2014, **118**, 7195–7202.

30 I. Horcas, R. Fernández, J. M. Gómez-Rodríguez, J. Colchero, J. Gómez-Herrero and A. M. Baro, *Rev. Sci. Instrum.*, 2007, **78**, 013705.

31 D. A. Case, T. A. Darden, T. E. Cheatham, C. L. Simmerling, J. Wang, R. E. Duke, R. Luo, R. C. Walker, W. Zhang, K. M. Merz, B. P. Roberts, S. Hayik, A. E. Roitberg, G. Seabra, J. M. Swails, I. Kolossváry, K. F. Wong, F. Paesani, J. Vanicek, R. M. Wo, A. Kovalenko and P. A. Kollman, *AMBER 12*, University of California, San Francisco (Computer program), 2012.

32 J. Wang, R. M. Wolf, J. W. Caldwell, P. A. Kollman and D. A. Case, *J. Comput. Chem.*, 2004, **25**, 1157–1174.

33 V. Maingi, V. Jain, P. V. Bharatam and P. K. Maiti, *J. Comput. Chem.*, 2012, **33**, 1997–2011.

34 J.-P. Ryckaert, G. Ciccotti and H. J. Berendsen, *J. Comput. Phys.*, 1977, **23**, 327–341.

35 W. Humphrey, A. Dalke and K. Schulten, *J. Mol. Graphics*, 1996, **14**, 33–38.

36 K. T. Nguyen, S. Syed, S. Urwyler, S. Bertrand, D. Bertrand and J.-L. Reymond, *ChemMedChem*, 2008, **3**, 1520–1524.

37 S. P. Amaral, M. H. Tawara, M. Fernandez-Villamarin, E. Borrajo, J. Martínez-Costas, A. Vidal, R. Riguera and E. Fernandez-Megia, *Angew. Chem., Int. Ed.*, 2018, **57**, 5273–5277.

38 J. W. Lee, H. J. Kim, S. C. Han, J. H. Kim and S.-H. Jin, *J. Polym. Sci., Part A: Polym. Chem.*, 2008, **46**, 1083–1097.

39 B. Fritzinger and U. Scheler, *Macromol. Chem. Phys.*, 2005, **206**, 1288–1291.

40 A. Lagunas, A. G. Castaño, J. M. Artés, Y. Vida, D. Collado, E. Pérez-Inestrosa, P. Gorostiza, S. Claros, J. A. Andrades and J. Samitier, *Nano Res.*, 2014, **7**, 399–409.

41 A. Lagunas, I. Tsintzou, Y. Vida, D. Collado, E. Pérez-Inestrosa, C. Rodríguez Pereira, J. Magalhaes, J. A. Andrades and J. Samitier, *Nano Res.*, 2017, **10**, 1959–1971.

42 P. K. Maiti, T. Çağin, G. Wang and W. A. Goddard, *Macromolecules*, 2004, **37**, 6236–6254.